https://doi.org/10.2352/CIC.2023.31.1.37

Multispectral imaging based on a multichannel LED system and RGB camera

Hui Fan, Ming Ronnier Luo*
State Key Laboratory of Extreme Photonics and Instrumentation, Zhejiang University, Hangzhou, China
****m.r.luo@zju.edu.cn***

Abstract

In this study, a multispectral imaging system with an RGB camera and a multichannel LED system was investigated. Firstly, it was proposed to generalize a previous method to optimize the flexible combinations of no more than three LED channels in each light source. The systems of 6-channel, 9-channel, and 12-channel were obtained, and their performances were compared with a typical 3-channel system under D65. Subsequently, the systems using single LED channels as light sources were explored. Two different methods (single-light and single-channel) were developed by selecting different numbers of the optimal lights or system channels. It was found the single-channel system outperformed the system using combined LED channels in terms of the spectral reconstruction accuracy. However, it should be noted the single-channel system required significantly more captures than the method by combining three channels in a light.

1. Introduction

Multispectral imaging aims to get the spectral reflectance or spectral radiance of each pixel in an image, providing the intrinsic characteristics of surface colors independent of the illuminant and observer conditions. It has great advantages over the conventional imaging by a trichromatic camera. Therefore, it has been widely applied in various fields including biomedicine, agriculture, cultural heritage, remote sensing, object identification [1-4], etc. In the prior art, researchers have made significant progress in developing advanced techniques for accurate spectral reconstruction in multispectral imaging [5-7]. Different types of systems, including systems based on filter wheel, liquid crystal tunable filter (LCTF), stereo camera, single-shot system with filter arrays, LED-based system, have been proposed and compared [8, 9].

With the rapid development of LED technology, researches have investigated the optimal light sources for spectral reflectance reconstruction [10], and the simulation of camera responses of pre-filters [11] using a multichannel LED system. This system has also been widely applied in the multispectral imaging [12-19]. Typically, it involves a multichannel LED system in conjunction with either a monochrome camera [12, 13] or trichromatic (RGB) camera [14-20].

Among the previous studies using RGB camera, researchers [15-17, 20] adopted a strategy to combine three optimal LED channels selected from three wavelength regions in each light source. The LED combinations were optimized through exhaustive search. In this way, each light source consisted of three LED channels, and each capture by an RGB camera resulted in three-channel camera responses. The effectiveness of this method has been verified. However, there were still some limitations. The exhaustive search method had a high cost and might be inapplicable when the number of LED channels was too large. Furthermore, in previous studies, the LED channels were typically grouped into R, G, and B categories according to their peak wavelengths and the wavelengths of intersections of camera spectral sensitivities. This grouping method might not be suitable for some broadband LED channels and could impose restrictions on the final performance of spectral reconstruction.

Meanwhile, we noticed that few studies have explored the feasibility of multispectral imaging by capturing images under single-channel LED light sources using an RGB camera. This approach required more captures compared to the method of combining each three LED channels in a light source. However, in theory, using N single LED channels in conjunction with an RGB camera could generate camera responses of $3*N$ channels. This study aimed to address the following question: Will this approach yield higher spectral reconstruction accuracy compared to the "combined-channel" method?

This study focused on the multispectral imaging using a multichannel LED system and an RGB camera. First of all, we proposed a more generalized approach for the optimization of LED channel combinations by applying a simulated annealing algorithm. The restrictions on the LED groups were eliminated. The 6-channel, 9-channel, and 12-channel systems were obtained. Next, we explored the systems using single LED channels as light sources. Two different methods, named as *single-light* and *single-channel*, were proposed with the aim of selecting different numbers of optimal LED lights or system channels. It was found the *single-channel* method achieved the highest accuracy among the three systems. However, this system required the greatest number of captures.

2. Method

System

Figure 1 illustrates the multispectral imaging system employed in this study. The system includes an LED viewing cabinet equipped with multiple LED channels and an RGB camera. Both can be controlled by a computer. Within the cabinet, a test chart is positioned and captured by the camera under each of the designed light sources.

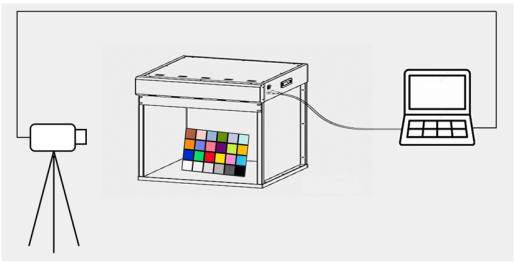

Figure 1. *Visualization of the multispectral imaging system.*

Combination of LED channels

The previous studies [15-17, 20] divided the LED channels into three groups, and each light source was the combination of three channels selected from each group. Then each capture would result in three-channel camera responses. In this study, we extended this method by removing the restrictions of channel grouping, allowing for more flexible combinations. Moreover, unlike previous studies

that strictly limited the number of LED channels in a light source to be three, we allowed flexibility in this number. Each light source was designed to contain 1~3 optimal LED channels. This was because, for some broadband channels, a single LED channel together with an RGB camera was sufficient to produce a three-channel response, making it unnecessary to include three LED channels in total.

The combinations of LED channels were optimized by a simulated annealing algorithm [21]. This algorithm simulated the process of annealing of a thermodynamic system, and searched for the state with the minimum energy. This method cannot guarantee to obtain the globally optimal solution, but can reduce the possibility to be trapped in a local optimal solution. This study aimed to minimize the spectral reflectance reconstruction error. The spectral reconstruction method was a simple linear regression method [22]. This method learned the transform matrix between the camera responses and spectral reflectance from the training samples, and was applied to the test samples to reconstruct the reflectance. The objective function was a colorimetric and spectral combined metric (CSCM) [21] as in Eq.(1). The colorimetric metric was the color difference CIEDE2000 (ΔE_{00}) [23] calculated using CIE 1931 standard observer under CIE D65. The spectral metrics included RMSE (Root Mean Square Error) and GFC (Goodness of Fit Coefficient). The coefficients a, b, and c were the weights of different metrics. In this study, we set a=b=c=1.

$$CSCM = a * \ln\left(1 + 1000(1 - GFC)\right) + b * \Delta E_{00} + c * 100 * RMSE \quad (1)$$

The optimizations with different numbers of light sources (2, 3, and 4) were conducted, corresponding to 6-channel, 9-channel, and 12-channel systems, respectively.

Single LED light/channel

In this section, each single LED channel was treated as an individual light source. Three-channel camera responses could be obtained under each light source. By repeating this process for all the N LED lights, a total of 3*N-channel camera responses could be obtained. Two different methods were tested, named as *single-light* and *single-channel*, respectively. The difference between them was in the selection process, i.e., either to select the optimal lights or to select the optimal system channels. Figure 2 shows the flowchart of the two methods.

In the *single-light* method, different numbers of the optimal lights were selected from the entire set of N lights. The effective spectral sensitivities of the system were determined by multiplying the camera spectral sensitivities with the spectral power distribution (SPD) of light. As shown in Figure 2(a), each LED light corresponded to three-channel effective sensitivities. However, due to the narrowband features of some LED lights, some of the resulting sensitivities had quite low responses, and some sensitivities had similar shapes only with intensity difference. These channels contributed little to the spectral reconstruction, and instead would lead to the accumulations of noise. As a result, it was decided to remove such system channels based on the following principles.

1. For all the 3*N system channels, calculate the GFC between each pair of effective sensitivities, and remove the one with lower sensitivity in the paired comparison of GFC>0.95.

2. For the three effective sensitivities in the same LED light, remove those with peak intensity lower than 20% of the maximum one.

After the removing process, each LED light could correspond to 0 to 3 effective channels. Then the optimal K lights were selected with the objective of minimizing the CSCM. The effect of the number of lights on the accuracy of spectral reconstruction was investigated.

In the *single-channel* method, as shown in Figure 2(b), the 3*N channels were mixed together, and the system was directly regarded as a 3*N-channel system, ignoring the interconnection between the three-channel responses in a light. Different numbers of the optimal channels were directly selected from the total 3*N channels. Again, the minimized objective was the CSCM of the validation set. In this method, the system channels with low/similar sensitivities were not preliminarily removed, since these channels would not be prioritized by the optimization algorithm.

For both methods, the simulated annealing algorithm was applied for the optimal light/channel selection.

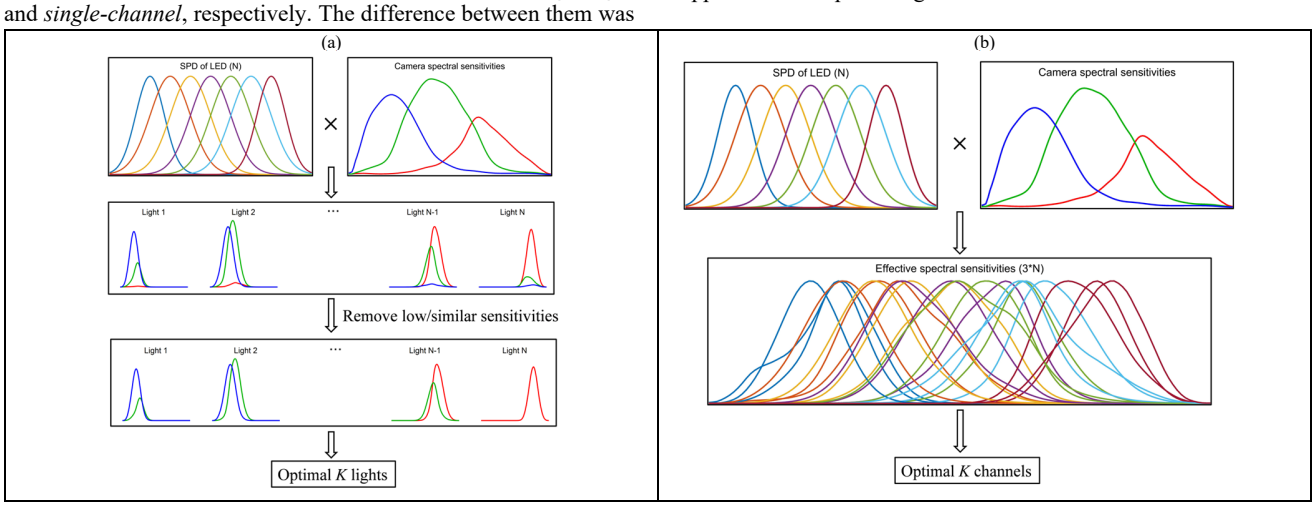

Figure 2. *The illustrations of the proposed methods, (a) single-light, (b) single-channel.*

3. Experiments

In this study, a Thouslite LEDView® viewing cabinet was used. It was equipped with a spectrum tunable LED system with 14 channels within the visible range. Figure 3 shows the normalized SPDs of the LED channels. The RGB camera was a Digital Single Lens Reflex (DSLR) camera, Canon 650D. Figure 4 plots the camera spectral sensitivities calibrated by a monochromator. Prior to the experiment, the linearity of the camera was verified by capturing the six neutral patches on the MCCC under D65.

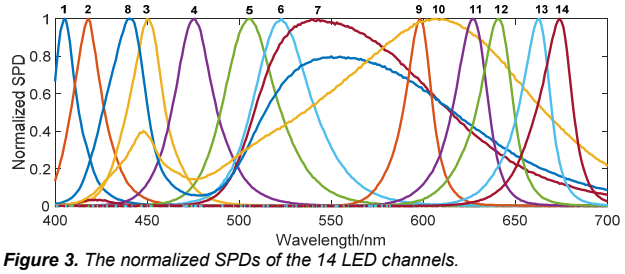

Figure 3. *The normalized SPDs of the 14 LED channels.*

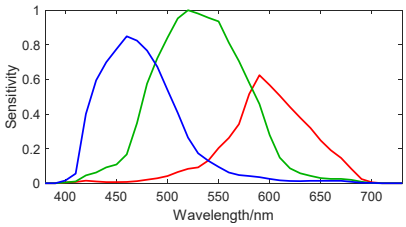

Figure 4. *The camera spectral sensitivities.*

The X-Rite Macbeth ColorChecker Chart (MCCC) served as the training dataset for spectral reflectance reconstruction. The X-Rite ColorChecker Digital SG (140 colors) were used as the validation dataset. The testing datasets included a DigiEye calibration chart DigiTizer (240 colors) and six hyperspectral images selected from two databases, CAVE [24] and Hyperspectral Images of Natural Scenes [25]. The hyperspectral images were only tested in the simulated experiment. The ground truth spectral reflectance of the charts was measured by a spectrophotometer Datacolor SF600.

Combination of LED channels

In the simulated experiment, random Gaussian noise with a Signal to Noise Ratio (SNR) of 40dB was added to the camera responses. The combinations of LED channels were optimized following the method in Section 2. The numbers of light sources were 2, 3, and 4, corresponding to 6-channel, 9-channel, and 12-channel systems, respectively. When tested by the hyperspectral images, considering the Bayer pattern of the RGB camera, a simple bilinear interpolation demosaic method was employed.

In the practical experiment, based on the optimization results, the corresponding LED channels were selectively activated in each light source. The SPDs of the lights were measured by a JETI-Specbos 1211 spectroradiometer on a white plate. The color charts were placed on a holder with a fixed angle of 60° in the center of the viewing cabinet. The camera was used to capture the color chart with an illumination/viewing geometry of 60°/0°. It was decided not to use 45°/0° geometry due to the significant specular reflections of the semi-glossy SG chart in that configuration. During the experiment, the focus, ISO, and exposure time of the camera were adjusted to their optimal settings and then fixed, to ensure that no overexposure occurred. The RGB camera was used to capture the images of color charts under a matched D65 light, and each of the optimized lights. The camera responses were extracted from the RAW images. Meanwhile, a white board was captured for the illumination uniformity correction, and a dark image was captured to subtract the dark noise.

Single LED light/channel

In this method, for the color charts, we only performed the practical experiment and did not include a simulation experiment. The experimental condition remained consistent with those described in the previous section. Images of the color charts were captured under each of the 14 individual LED lights. The light/channel selection process was guided by the camera responses measured in the practical experiment, with the objective of minimizing the CSCM of the validation dataset. The optimal lights/channels were selected following the previously described *single-light* and *single-channel* methods, respectively.

After determining the optimal lights or channels, the systems were further tested by the hyperspectral images in simulations. Again, random Gaussian noise with SNR of 40dB was added, and a bilinear interpolation method was employed for demosaic process.

4. Results

Combination of LED channels

Table 1 lists the selected combinations of LED channels for different numbers of light sources. The LED channels were labeled following the serial numbers as given in Figure 3. It was observed that five of the channels (No 1, 3, 7, 11, and 14) were present in all the cases with different numbers of lights. This suggests that these channels might be critical for the accurate spectral reconstruction.

Table 1. The results of LED channel combination selection.

	Light1	Light2	Light3	Light4
6-channel	[14,5,3]	[7,1,11]	/	/
9-channel	[14,3,4]	[11,1,9]	[7,6]	/
12-channel	[12,6,2]	7	[1,9,11]	[14,3,4]

Table 2 lists the spectral reconstruction error of D65 light and three optimized systems in the simulated experiment. The system under D65 could be regarded as a typical 3-channel system. The colorimetric metric ΔE_{00} was calculated under CIE D65, A, and F11. It was found that the spectral reconstruction error initially decreased and then became nearly stable as the number of system channels increased. The RMSE deceased by more than a half when transitioning the system from 3-channel to 6-channel, and slightly decreased for the 9-channel system. However, with more numbers of system bands, due to the accumulation of system noise, the accuracy could not be further improved.

Table 2. The spectral reconstruction error of the *combined-light* method in the simulated experiment.

Testing samples	System	ΔE_{00}			RMSE	GFC
		D65	A	F11		
SG	D65	2.90	3.12	3.54	0.0359	0.9857
	6-channel	2.05	2.01	2.79	0.0161	0.9934
	9-channel	1.42	1.45	2.24	0.0155	0.9913
	12-channel	1.40	1.39	2.33	0.0153	0.9885
DigiTizer	D65	2.32	2.54	2.71	0.0311	0.9844
	6-channel	1.70	1.63	2.29	0.0152	0.9917
	9-channel	1.17	1.18	1.83	0.0149	0.9903
	12-channel	1.16	1.13	1.86	0.0150	0.9891

Figures 5 (a)~(c) plot the measured SPDs of the lights with different numbers. Figures 5 (d)~(f) plot the normalized effective spectral sensitivity functions of the systems with different channels. The effective spectral sensitivity functions were obtained by multiplying of the light SPDs with the camera spectral sensitivities.

Overall, it can be observed that the peak wavelengths of the effective sensitivities spanned the entire wavelength range.

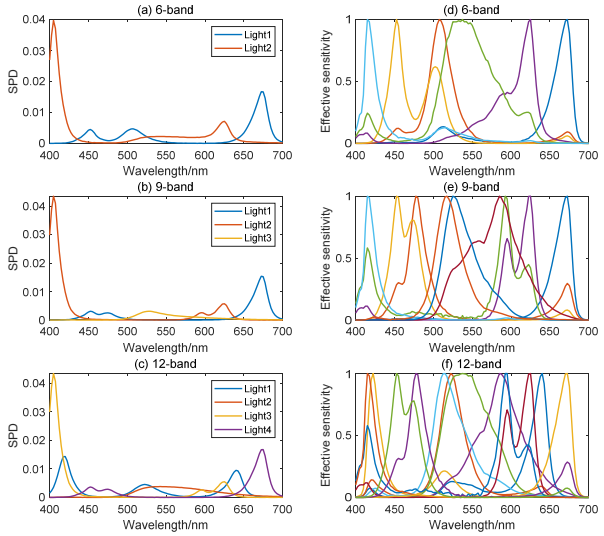

Figure 5. *(a)(b)(c) The measured SPDs of the light sources with numbers of 2, 3, and 4. (d)(e)(f) The effective spectral sensitivities of the 6-channel, 9-channel, and 12-channel systems.*

Table 3 lists the spectral reconstruction error in the practical experiment. The overall trend of the results was similar to that observed in the simulation. It was noticed in some cases the trends of the three metrics were inconsistent. For example, when tested by DigiTizer, the RMSE significantly decreased from D65 to the 6-channel system, while the ΔE_{00} under D65 slightly increased. This might be explained by the possibility that the metamers of the test samples were obtained under D65, leading to a small color difference under D65 but a relatively large RMSE.

Table 3. The spectral reconstruction error of the *combined-light* method in the practical experiment.

Testing samples	System	ΔE_{00}			RMSE	GFC
		D65	A	F11		
SG	D65	2.89	3.34	3.53	0.0409	0.9881
	6-channel	2.51	2.54	2.67	0.0254	0.9970
	9-channel	2.15	2.19	2.32	0.0238	0.9972
	12-channel	2.01	1.96	2.83	0.0196	0.9972
DigiTizer	D65	1.78	2.18	2.24	0.0337	0.9872
	6-channel	1.82	1.88	1.93	0.0221	0.9944
	9-channel	1.75	1.81	1.84	0.0203	0.9952
	12-channel	1.73	1.68	2.43	0.0228	0.9957

Single-light method

Capturing the 14 single LED lights resulted in 42-channel camera responses. After removing those with similar or low sensitivities according to the principles proposed in the *single-light* method, there were 20 system channels remained. Figure 6 plots the remained effective sensitivities in each light.

Figure 7 plots the spectral reconstruction error with varying numbers of lights in the *single-light* method. The error metrics, ΔE_{00} under D65, RMSE, and GFC, were tested on both color charts. It was found with the increase of numbers of lights, the reconstruction errors initially decreased and then increased. This implied that more numbers of lights, and thus more numbers of system channels, did not necessitate higher accuracy of spectral reconstruction. When the number of lights was 8, the CSCM reached its minimum. The optimal lights were No.1, 3 , 5, 6, 8, 11, 12, and 14, resulting in a 12-channel system. Figure 8 plots the effective spectral sensitivities of the 12-channel system.

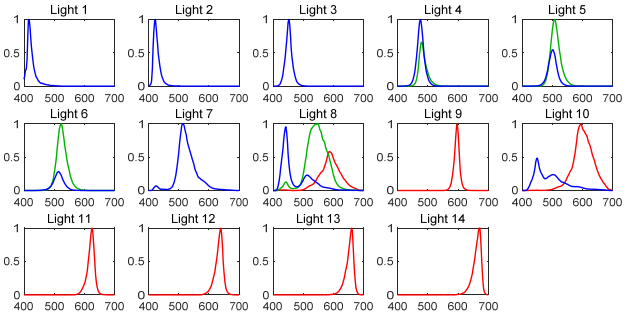

Figure 6. *The effective spectral sensitivities in each light after removing the low-response and similar sensitivities.*

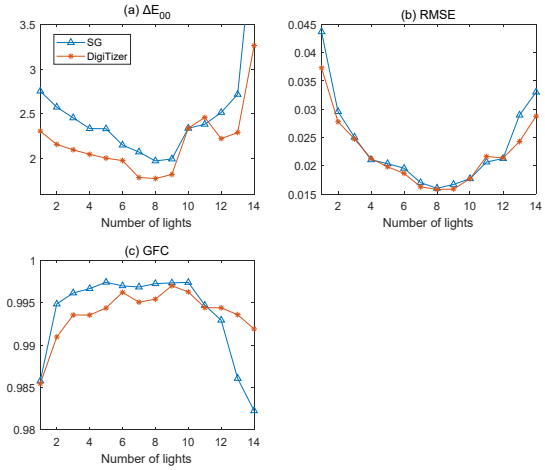

Figure 7. *The spectral reconstruction error with different numbers of lights tested by SG and DigiTizer charts, in terms of (a) ΔE_{00} under D65, (b) RMSE, (c) GFC.*

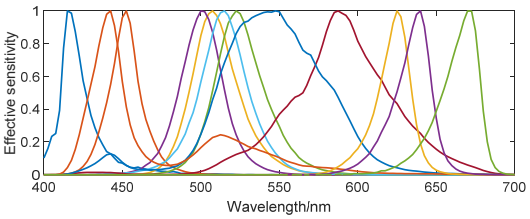

Figure 8. *The effective spectral sensitivities of the optimized 12-channel system in the single-light method.*

Single-channel method

Figure 9 plots the spectral reconstruction error with different numbers of system channels (from 3 to 42) in the *single-channel* method. It was found with the increase of system channels, the reconstruction accuracy first decreased, then increased, and finally exhibited oscillations. This observation verified that the 42-channel system was highly redundant due to the existence of some low-response and similar channels. Therefore, it was necessary to select the optimal channels from them.

When the number of system channels was 12, the CSCM reached its minimum. Figure 10 plots the effective spectral sensitivities of the 12-channel system. The peak wavelengths of these channels generally spanned across the visible range. Among the selected channels, there were two pairs resulted from the same LED lights. Therefore, this 12-channel system required to capture under 10 different lights.

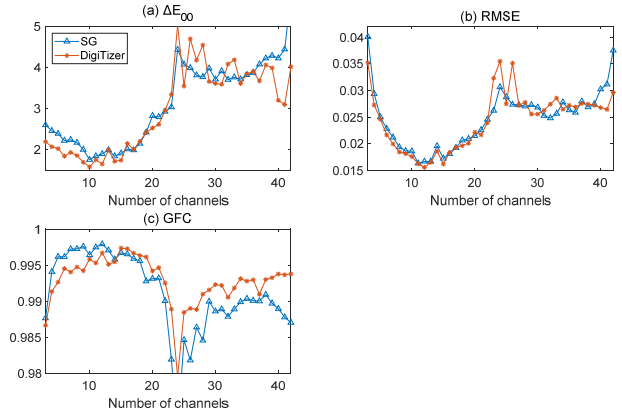

Figure 9. *The spectral reconstruction errors with different numbers of system channels tested by SG and DigiTizer charts, in terms of (a) ΔE_{00} under D65, (b) RMSE, (c) GFC.*

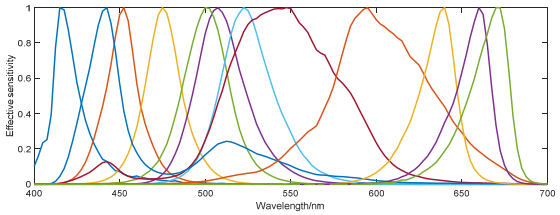

Figure 10. *The effective spectral sensitivities of the optimized 12-channel system in the single-channel method.*

Table 4. The spectral reconstruction errors of the *single-light* and *single-channel* methods in the practical experiment.

Testing samples	System	ΔE_{00}			RMSE	GFC
		D65	A	F11		
SG	*single-light*	1.97	1.86	2.22	0.0160	0.9972
	single-channel	1.90	1.88	1.92	0.0167	0.9979
DigiTizer	*single-light*	1.77	1.62	2.02	0.0158	0.9954
	single-channel	1.66	1.60	1.61	0.0156	0.9967

Table 4 summarizes the results of spectral reconstruction of the *single-light* and *single-channel* methods. Overall, it can be observed that the *single-channel* method achieved slightly higher accuracy than the *single-light* method. This result was reasonable since the *single-channel* method aimed to search the optimal results among all the combinations of 42 channels, which inherently included the solutions of *single-light* method. However, it should be noted that the 12-channel system obtained with *single-channel* method required two more capture times.

When comparing the results with those of the *combined-channels* as in Table 3, it was found the 12-channel system obtained through *single-channel* method outperformed the 12-channel system using combined channels. The *single-channel* method yielded significantly smaller RMSE, indicating higher accuracy in spectral reconstruction. When we looked at the effective spectral sensitivities of the two systems (Figure 5 and 10), it can be found the sensitivities of the *single-channel* method had single peak (except the one related to a double-peak LED channel), while those obtained with the combined channels had some obvious secondary peaks. In the *combined-channel* method, consider a light source composed of three different LED channels, each camera channel would respond to all the three LED channels, causing the total sensitivities to be not unimodal. This might have impact on the performance of spectral reconstruction. However, the method with combined channels required much fewer capture times than the *single-channel* method (4 vs 10). This approach had a great advantage of saving time in practical applications on multispectral imaging. Therefore, it seemed to be a trade-off between the spectral reconstruction accuracy and the system efficiency.

Another issue to be discussed was the difference in obtaining the two systems in the *combined-channel* and *single-channel* methods. The system with combined channels was optimized through simulations, and then tested in practical experiments. Due to the incomplete noise model, there might be discrepancies between the simulated and practical results. So that the results in practical experiment might not be the global optimal ones. While for the *single-channel* system, we directly selected the optimal channels based on the measured camera responses of the validation set. It seemed somewhat "unfair" to compare the two systems optimized either by simulations or real measurements. However, it was exactly the advantage of the *single-channel* method. This method did not require the prior knowledge of camera spectral sensitivities or even the SPDs of LED lights. The channel selection was solely based on the practical measurements on the validation dataset. The subsequent testing on the test dataset has verified the superiority of this method.

Simulation on hyperspectral images

The systems with combined channels and single channels were further tested in the simulations on hyperspectral images. Figure 11 illustrates the reconstructed RMSE of different systems, including D65 (3-channel), the 12-channel systems with *combined-channel* and *single-channel* methods. The mean RMSE values were provided at the bottom of each figure. The demosaic process in hyperspectral images could introduce more system noise compared to the previous simulations on color charts (uniform color patches), but it was closer to the real-world scenarios using an RGB camera.

The results demonstrated that both the 12-channel systems had significant improvements on the accuracy of spectral reconstruction compared to the 3-channel system under D65. Moreover, the 12-channel system obtained through the *single-channel* method slightly outperformed the system using combined channels. More advanced demosaic algorithms could be applied to investigate the possibility to further increase the spectral reconstruction accuracy.

5. Conclusions

In this study, the multispectral imaging system based on a multichannel LED system and an RGB camera was studied. First, we proposed to generalize a previous method of combined LED channels. A simulated annealing algorithm was applied to optimize the flexible combinations of LED channels. Each light was designed to include no more than three LED channels. In this method, we respectively obtained 6-channel, 9-channel, and 12-channel systems. Then the system with individual LED channels were explored. Two methods (*single-light* and *single-channel*) were proposed to select the optimal LED lights or system channels. It was found the 12-

channel system obtained by *single-channel* method performed slightly better than the *single-light* method. Furthermore, the *single-channel* system significantly outperformed the *combined-channel* system in the practical experiment on test charts, and slightly outperformed the *combined-channel* system in the simulations on hyperspectral images. However, the *single-channel* method required much more captures (10) compared to the *combined-channel* method (only 4). As a result, a trade-off existed between the spectral reconstruction accuracy and the system efficiency. In the future work, additional test color samples, and more advanced spectral reconstruction and channel selection methods will be investigated. Using more sophisticated spectral reconstruction algorithms, the resulting optimal system channels might be different.

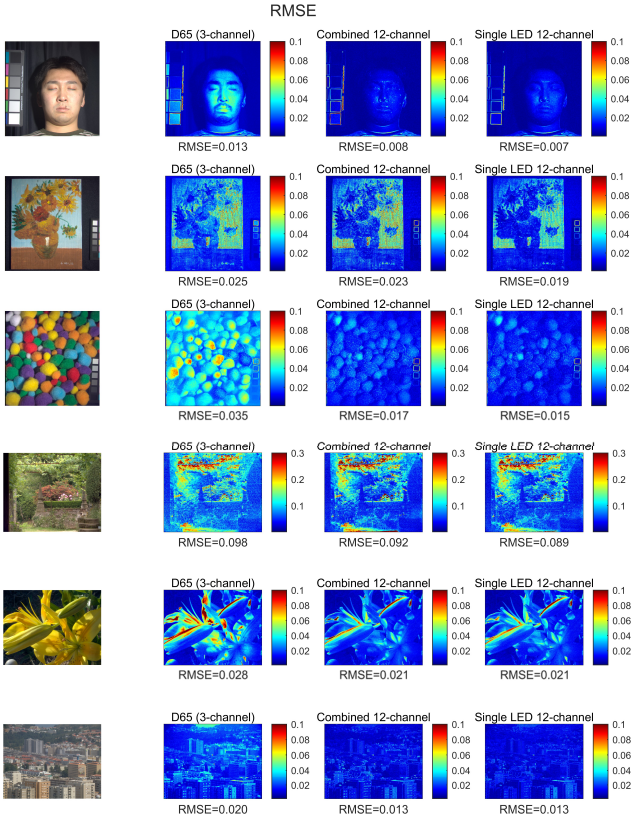

Figure 11. *The RMSE of different systems in the simulations on hyperspectral images.*

References

[1] M. B. Bouchard, B. R. Chen, S. A. Burgess, and E. M. C. Hillman, "Ultra-fast multispectral optical imaging of cortical oxygenation, blood flow, and intracellular calcium dynamics," *Optics Express,* vol. 17, no. 18, pp. 15670-15678, 2009.

[2] J. Qin, K. Chao, M. S. Kim, R. Lu, and T. F. Burks, "Hyperspectral and multispectral imaging for evaluating food safety and quality," *Journal of Food Engineering,* vol. 118, no. 2, pp. 157-171, 2013.

[3] A. Pelagotti, A. D. Mastio, A. D. Rosa, and A. Piva, "Multispectral imaging of paintings," *IEEE Signal Processing Magazine,* vol. 25, no. 4, pp. 27-36, 2008.

[4] F. Hu, M. Zhou, P. Yan, K. Bian, and R. Dai, "Multispectral Imaging: A New Solution for Identification of Coal and Gangue," *IEEE Access,* vol. 7, pp. 169697-169704, 2019.

[5] Y.-T. Lin and G. D. Finlayson, "A Rehabilitation of Pixel-Based Spectral Reconstruction from RGB Images," *Sensors*, vol. 23, no. 8,

[6] J. Liang, K. Xiao, M. R. Pointer, X. Wan, and C. Li, "Spectra estimation from raw camera responses based on adaptive local-weighted linear regression," *Optics Express,* vol. 27, no. 4, pp. 5165-5180, 2019.

[7] H. A. Khan, J.-B. Thomas, J. Y. Hardeberg, and O. Laligant, "Multispectral camera as spatio-spectrophotometer under uncontrolled illumination," *Optics Express,* vol. 27, no. 2, pp. 1051-1070, 2019.

[8] R. Shrestha and J. Y. Hardeberg, "Evaluation and comparison of multispectral imaging systems," in *22th color and imaging conference*, 2014, pp. 107-112.

[9] R. Shrestha and J. Y. Hardeberg, "Quality comparison of multispectral imaging systems based on real experimental data," presented at the The 13th International AIC Congress, 2015.

[10] L. X. Wang, A. Sole, J. Y. Hardeberg, and X. X. Wan, "Optimized light source spectral power distribution for RGB camera based spectral reflectance recovery," *Optics Express,* vol. 29, no. 16, pp. 24695-24713, 2021.

[11] Y. Zhu and G. D. Finlayson, "Matched illumination: using light modulation as a proxy for a color filter that makes a camera more colorimetric," *Optics Express,* vol. 30, no. 12, pp. 22006-22024, 2022.

[12] R. Shrestha, J. Y. Hardeberg, and C. Boust, "LED Based Multispectral Film Scanner for Accurate Color Imaging," in *2012 Eighth International Conference on Signal Image Technology and Internet Based Systems*, 2012, pp. 811-817.

[13] H. Liu, J. Sticklus, K. Köser, and H.-J. T. Hoving, "TuLUMIS - a tunable LED-based underwater multispectral imaging system," *Optics Express,* vol. 26, no. 6, pp. 7811-7828, 2018.

[14] M. Parmar, S. Lansel, and J. Farrell, "An LED-based lighting system for acquiring multispectral scenes," presented at the Proceedings of SPIE - The International Society for Optical Engineering, 2012.

[15] R. Shrestha and J. Y. Hardeberg, "Multispectral imaging using LED illumination and an RGB camera," in *21st Color and Imaging Conference*, 2013, pp. 8-13.

[16] R. Shrestha and J. Y. Hardeberg, "An experimental study of fast multispectral imaging using LED illumination and an RGB camera," in *23th Color and Imaging Conference*, 2015, pp. 36–40.

[17] M. Safdar, M. R. Luo, Y. Wang, and X. Liu, "Multispectral Imaging System based on Tuneable LEDs," presented at the Multispectral Color Science (MCS) Symposium, 2015.

[18] J. I. Park, M. H. Lee, M. D. Grossberg, and S. K. Nayar, "Multispectral Imaging Using Multiplexed Illumination," in *2007 IEEE 11th International Conference on Computer Vision*, 2007, pp. 1-8.

[19] J. M. DiCarlo, F. Xiao, and B. A. Wandell, "Illuminating illumination," in *the 9th Color Imaging Conference*, 2001, pp. 27–34.

[20] O. Kuzio and S. Farnand, "Comparing Practical Spectral Imaging Methods for Cultural Heritage Studio Photography," *Journal on computing and cultural heritage,* vol. 16, no. 1, pp. 1-13, 2023.

[21] M. A. López-Álvarez, J. Hernández-Andrés, J. Romero, and R. L. Lee Jr, "Designing a practical system for spectral imaging of skylight," *Applied Optics,* vol. 44, no. 27, pp. 5688-5695, 2005.

[22] R. Penrose, "A generalized inverse for matrices," *Mathematical proceedings of the Cambridge Philosophical Society,* vol. 51, no. 3, pp. 406-413, 1955.

[23] "Colorimetry Part 6: CIEDE2000 Color-Difference Formula," *ISO/CIE 11664–6:2014(E)*.

[24] F. Yasuma, T. Mitsunaga, D. Iso, and S. K. Nayar, "Generalized Assorted Pixel Camera: Postcapture Control of Resolution, Dynamic Range, and Spectrum," *IEEE Transactions on Image Processing,* vol. 19, no. 9, pp. 2241-2253, 2010.

[25] D. H. Foster, K. Amano, S. M. C. Nascimento, and M. J. Foster, "Frequency of metamerism in natural scenes," *Journal of the Optical Society of America A,* vol. 23, no. 10, pp. 2359-2372, 2006.

Author Biography

Hui Fan received her BS in Optical Engineering from Nankai University (2020) and she is now a PhD student supervised by Professor Ming Ronnier Luo at Zhejiang University. Her research work is on camera spectral calibration and multispectral imaging.